



Sacred Heart Institute
third degree
355 Naamsesteenweg
3001 HEVERLEE

Wind tunnel

Design and construction of an open wind tunnel

Martin Espel
Wolf Vierbergen
Kobe Vlasselaer
6 Technology-Sciences
GIP

School year 2019-2020



Sacred Heart Institute
third degree
355 Naamsesteenweg
3001 HEVERLEE

Wind tunnel

Design and construction of an open wind tunnel

Martin Espel
Wolf Vierbergen
Kobe Vlasselaer
6 Technology-Sciences
GIP

School year 2019-2020
3

PREFACE

This integrated test is about designing, building and testing a wind tunnel. This paper was written within the framework of the GIP of 6 TW in the Sacred Heart Institute Heverlee. We worked on this paper from September to April.

Together with our mentor, Ludo Verluyten, we formulated the research questions. Construction was slow in the beginning due to problems with ordering the parts, but it has been nicely finished. In this way we were also able to answer the research question. While writing, we could always ask our mentor, Ludo Verluyten, our questions so that we could continue smoothly.

We would like to thank our mentor for always supporting us in recent months. In addition, our Dutch teacher for improving each version. We would also like to thank Harm Ubbens for his tips and feedback and especially for helping where necessary at the beginning of the research. Without this help, this research would not have been possible.

We would also like to thank all the friends and family who supported us mentally and financially during the design, build, testing and writing of this paper. Thanks to them we can successfully close this investigation.

We wish you a pleasant reading experience.

Kobe Vlasselaer
Martin Espel
Wolf Vierbergen

Leuven, February 2020

Contents

PREFACE.....	5
INTRODUCTION	8
1 literature study	9
1.1 Aerodynamics.....	9
1.1.1 History of aerodynamics	9
1.1.2 Importance of an aerodynamic object	10
1.2 Determining Laminar or Turbulent Flow.....	10
1.3 Bernoulli's Law	10
1.4 Application: Operation of an aircraft	11
1.4.1 Propulsion	12
1.4.2 Resistance	12
1.4.3 Elevator	13
1.4.4 Angle of view	15
1.5 Determination of the wind speed.....	16
1.6 Wind tunnel	17
1.6.1 Definition and principle	17
1.6.2 Types of wind tunnels	17
1.6.3 Objective of the project	18
2 Materials and Methods.....	19
2.1 Requirements and components of an open wind tunnel.....	19
2.1.1 Honeycomb.....	19
2.1.2 Screens	20
2.1.3 The Funnel	21
2.1.4 The test section	23
2.1.5 Diffuser.....	24
2.1.6 Fans	25
2.2 Assembly of the wind tunnel.....	27
2.3 Materials for the construction of the wind tunnel	27
2.3.1 Additional production machines.....	27
3 Practical test	28
3.1 Wind tunnel design	28
3.2 Making laminar flow visible.....	29
3.3 Determining the airspeed	30
3.3.1 Components of the test set-up when determining the airspeed.....	30
3.3.2 Measurement of the air speed at maximum fan position.....	31
3.3.3 Airspeed Measurement at Predetermined Settings	32
3.4 Determination of the lift of a wing at different angles of attack.....	33
3.4.1 Procedure for measuring lift on a wing.....	33
3.4.2 Determination of the lift force and lift coefficient as a function of the angle of attack	34
3.4.3 Lift Force and Lift Coefficient as a Function of Airspeed.....	36
4 General decision	38
5 Literature list	39
6 List of Figures	41
7 List of tables	42

INTRODUCTION

Our integrated test (plaster) is about wind tunnels. We absolutely wanted to make our plaster on aerodynamics. We think it is a pity that aerodynamics is not part of the curriculum of secondary education and that is why we wanted to base our plaster on it.

The aim of our plaster is to build a wind tunnel that works so that we can do tests on it. We want to prove that it is possible to generate laminar power with our self-built wind tunnel. It was a long project with many setbacks and additional problems that we did not expect.

Our integrated test also includes an experimental part: we did tests in our wind tunnel and tried to find the optimal angle and shape for a wing so that it experiences as little air resistance as possible.

We looked for our information on the internet and we also visited Bike Valley. They have built a wind tunnel to test the attributes of cycling (kits, shape of bicycle and helmets) so that the cyclist suffers as little as possible from air resistance. There they gave us many tips for the shape and materials of our wind tunnel.

For us it was a very interesting and instructive experience to build a wind tunnel and we hope that you will have an instructive and enjoyable experience reading our integrated test.

1 literature study

1.1 Aerodynamics

Aerodynamics is the science that describes the movement of gases and liquids. It is part of the field of fluid mechanics. Describing the flow behavior of a liquid or gas can relate to flow in free space or to a body such as an aircraft wing [4].

1.1.1 History of Aerodynamics

The science of aerodynamics has only existed since the 17th century. Before that, however, people had already used the wind for a long time, such as in a sailing boat and a windmill.

The first person to develop a theory of air resistance was Isaac Newton. He was followed by Daniel Bernoulli, who found a relationship between pressure, density and flow velocity in an incompressible flow. After that, knowledge about aerodynamics progressed at a rapid pace thanks to contributions from Leonhard Euler and Sir George Cayley, among others.

In the early 18th century, Benjamin Robins began measuring air resistance with a whirling arm. Frank H. Wenham also experimented with this, but the results were not satisfactory. This is how the idea of a wind tunnel came about. In 1871 the first wind tunnel was built by the Briton Francis Herbert Wenham, allowing accurate measurements of aerodynamic forces. The experiments he performed were related to lift and drag [17]. A replica of this first wind tunnel can be found in figure 1.



Figure 1: Replica of the first wind tunnel

German Otto Liliental was the first person to fly in a glider. He succeeded with a new design of the wings, which had a thin and curved airfoil so that they would produce high lift and low drag. Thanks to Liliental's new wings and their own research in their wind tunnel, the Wright brothers made their first successful flight in a powered aircraft on December 17, 1903. [4]

1.1.2 Importance of an aerodynamic object

Air is a matter that exerts a force on an object when it flows past it. During the process, the air sticks to the object a bit, which we call air resistance. For an object that is as aerodynamic as possible, the air resistance must be minimal. The wind therefore sticks a bit on the object, but that does not happen a little above the object. So there is a difference in speed between the air that hits the object (lower airflow) and the air that flows a little above it (upper airflow). This creates a boundary layer between the two different air flows. If the lower airstream separates from the object and collides with the upper airstream, turbulent flow is created. Due to the collision, the wind particles form a swirling trajectory, which causes a lot of air resistance.

In order to obtain an object that is as aerodynamic as possible, it is therefore necessary to ensure that the airflow sticks to the object and does not come loose from it or as little as possible. So one tries to avoid corners and to obtain a nice smooth layer. [19]

1.2 Determination Laminar or turbulent flow

Osbourne Reynolds defined the Reynolds number in 1883. He was an Irish physicist who was mainly concerned with hydraulics and hydrodynamics.

The Reynolds number is a dimensionless quantity used to determine whether a flow is laminar or turbulent. A dimensionless number means that the number has no unit. The number can be calculated using the following formula:

$$Re = \frac{\rho \cdot v \cdot D}{\mu}$$

Whereby:

- ρ = the density in kg/m³ • v
- = the speed in m/s.
- D = characteristic length in m.
- μ = the dynamic viscosity expressed in kg/ms

If the Reynolds number has a low value, you have laminar flow, and if the value is high, the flow is turbulent. For example, with flow in tubes you have laminar flow if the Reynolds number has a value below 2300 and you have turbulent flow if the Reynolds number has a value above 3500. If the number has a value between 2300 and 3500, it depends of various factors such as wall roughness whether you have turbulent or laminar flow. [8, 25 & 37]

1.3 Bernoulli's law

Daniel Bernoulli was a Swiss physicist who lived in the 18th century. In 1725 he moved to Saint Petersburg in Russia where he went to study at the newly founded academy. There he met Leonard Euler with whom he would later work closely. Bernoulli's law describes the flow behavior of gases and liquids and gives a

explanation of the pressure change with altitude and speed changes. For example, he writes that the faster a gas or liquid passes an object, the lower the pressure on that object will be. Of course, the law also works the other way around, ie the slower a liquid or gas passes through an object, the greater the pressure on that object will be [34, 7]. Bernoulli derived a formula that uses the law of conservation of energy. The sum of the kinetic energy density (dynamic pressure), the gravitational pressure and the pressure equals a constant.

$$\frac{1}{2} \rho v^2 + \rho gh + p = \text{constant}$$

Of ρ = the density (kg/m³)
 v = the speed (m/s)
 g = the acceleration of gravity (m/s²)
 h = the height difference (m)
 p = the pressure (Pa)

Bernoulli's law applies under a number of conditions. These are the following:

1. Density is constant. The fabric must therefore not be compressed or stretched anywhere.
2. The fabric must not have internal friction. The viscosity should be zero.
3. The flow is stationary (= constant speed).

1.4 Application: Aircraft operation

Like every object on our earth, an airplane is attracted by gravity. In order to put an aircraft in the air, forces that counteract gravity must therefore be exerted. This force, which must ensure that an aircraft does not fall down, is also referred to as 'the lift'. This acting lift force must be greater than gravity and in the opposite direction.

In addition, an aircraft must be able to move in the air. Here too, the aircraft encounters an opposing force, namely the resistance of the air. In order to move in the air, the aircraft must therefore perform extra work, which is provided by the aircraft's engines.

Figure 2 illustrates the action of the various forces.



Figure 2: Forces on an aircraft

1.4.1 Propulsion

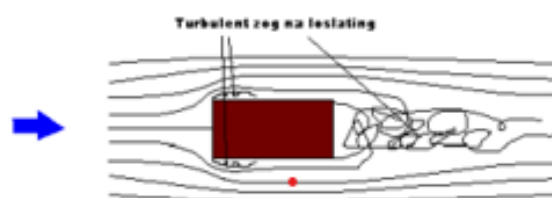
In order for an aircraft to propel in the air, it must exert forward thrust. There are two types of engines that can produce this thrust, propeller-driven or jet-powered engines.

In a propeller drive, a rotational movement of a propeller or airscrew is caused by a motor. The propeller rotates in the air and this creates a pressure difference at the front and rear of the propeller blades, creating a forward force. This force pushes the plane forward.

In jet propulsion, air is sucked into the front of a jet engine and then compressed by a compressor. The air is mixed with the fuel and when burned creates a large amount of heat. These heated gases will expand strongly at the rear as they leave the engine. The associated pressure differences cause the propulsive force. The propulsive force generated by the engine must be at least as great as the drag force of the air.

1.4.2 Resistance

When an object moves forward in the air, this object experiences a resistance from the air particles that opposes the forward movement. This aerodynamic force is a force caused by the object's interaction with the air. Air has a certain viscosity and will, as it were, stick to the object. This creates a speed difference between the air above the surface of the object and the air adjacent to the object. This causes a variation in flow. A laminar flow that offers little resistance can turn into a turbulent flow in which the air particles make rotational movements that increase the resistance. In addition, the air particles have a hard time moving along a sharp angle. A void is then created behind the block with turbulent flows that offer a lot of resistance,



Een blok in de strooming

Figure 3: turbulent flow at a block [39]

These turbulent flows must be avoided as much as possible because this means that the aircraft will have to develop more power to move forward. To reduce these turbulent flows, it will be necessary to ensure that the aircraft and wings adopt a shape that is more 'aerodynamic'. Among other things, sharp corners on the aircraft must be avoided. Scientists have been able to show that a wing/aircraft that has a teardrop shape will give the best results [19]. With this teardrop shape, the wing is rounded at the front and ends in a point at the back. This way the laminar flow is maintained as shown in figure no. 4. The droplet as shown in figure 4 is the most aerodynamic.

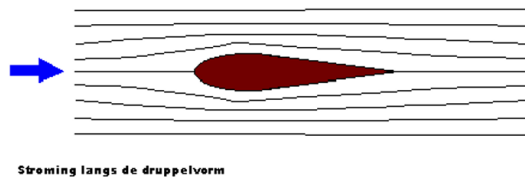


Figure 4: Currents along a drop shape (27)

In addition, the air molecules create a frictional force on the aircraft. It has been shown that when the surface of the aircraft is smooth, there is less friction than with a rough surface [19].

1.4.3 Elevator

To obtain lift in an aircraft, the upward force must be greater than the downward gravitational force, because according to Newton's second law, an object can only lift if the sum of all the forces acting on that object produces a net upward force. Several theories have been described to explain aircraft lift and some theories are more accepted than others. It is always important that lift can only be obtained when a fluid such as air is present, causing the wing to collide with the air molecules when the aircraft is moving forward.

In a first theory, Bernoulli's law is applied. The lift is generated by the specific asymmetric curvature of the wing which causes the flow to flow faster on top of the wing than under the wing. Because of the shape of the wing, the airflow will travel a greater distance at the top than at the bottom. This means that the air has to move faster from above over the wing. These airspeed differences are converted into pressure differences via Bernoulli's law. The greater the speed of the air, the lower the pressure (see Figure 5) [21].

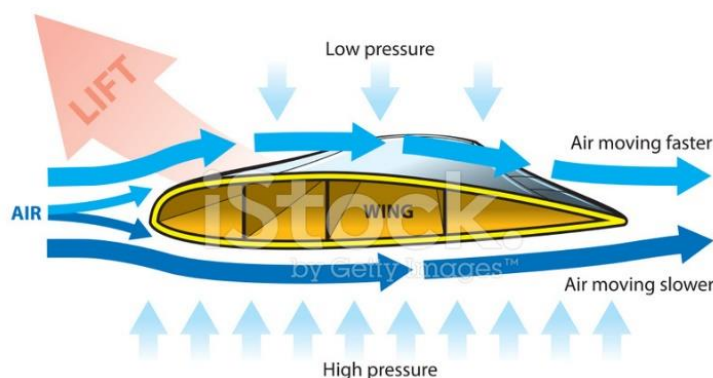


Figure 5: Pressure differences on a wing [21]

This means that the air pressure at the bottom of the wing is higher than at the top. These pressure differences therefore provide a vertical lift force upwards. This theory can be found in many textbooks, but this theory is not entirely correct. According to this theory, in order to gain lift, the wing must have an asymmetrical shape in which the air above the wing travels a longer distance than at the bottom of the wing. However, it has been shown that lift can also be created with wings with a symmetrical shape. In addition, planes can sometimes be seen flying upside down in aircraft shows. The air molecules will then become one

travel longer distance at the bottom compared to the top. These aircraft also remain suspended in the air and thus receive a lifting force upwards [26]

Another and currently more accepted explanation for lift force is the fact that due to the shape and angle a wing makes, the air will move in a downward direction. Due to Newton's second law, this will create a downward force on the air. This downward force then causes an upward force according to Newton's third law (action and reaction). So the wing exerts a downward force on the air and the air therefore exerts an upward force on the wing as shown in Figure 6.

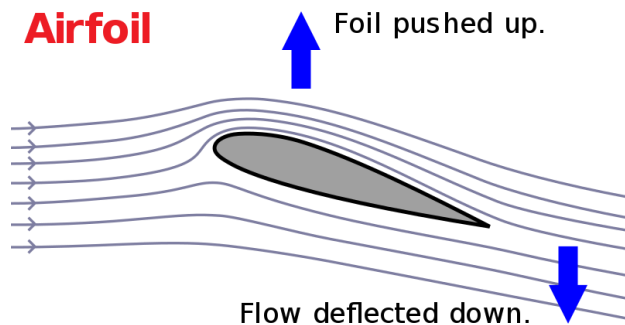


Figure 6: Downward and upward forces on a wing due to the flow of air [43]

In addition, due to the flow of air under the wing, an overpressure is generated at the underside of the wing compared to the top. These pressure differences then cause a lift force.

In addition, there is also the fact that extra lift can be created by the Coandă effect. When air collides with a surface, it tends to follow the shape of the surface. The forward motion of the aircraft thus creates an airflow that will follow the spherical shape of the wing. This will increase the airspeed and by Bernoulli's law the pressure above the wing will decrease. Which causes extra lift. This effect can be further enhanced by using extra flaps on the wing, as shown in figure 7

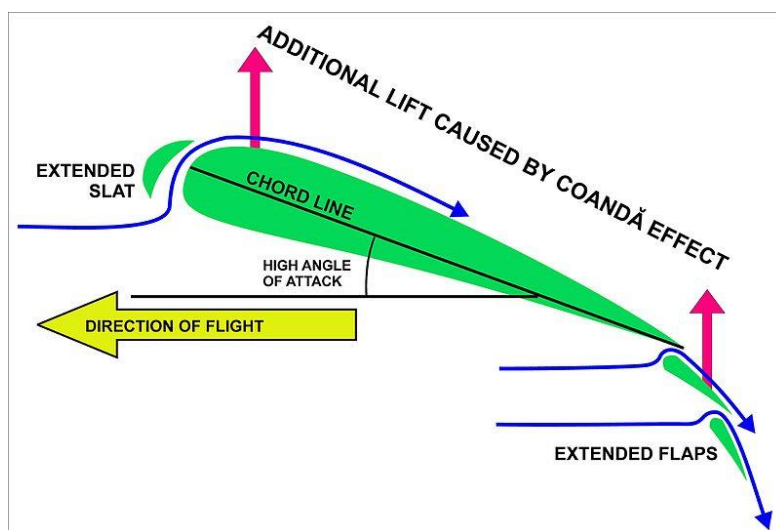


Figure 7: The Coanda effect on a wing [6])

1.4.4 angle

According to Bernoulli's law, the lift force is determined by the density of the air, the airspeed, the area of the wing and the lift coefficient as shown in the following formula [32]:

$$L = \frac{1}{2} \rho v^2 S C_L(\alpha)$$

Whereby:

L = elevator

ρ = the density of air in kg/m³

v = airspeed (m/s)

S = area of the wing in m²

$C_L(\alpha)$ = lift coefficient relative to the angle of attack - (figure 9)

This lift coefficient is determined by the angle the wing makes with respect to the airflow. This angle is also called the angle of attack. The determination of this angle of attack is shown in figure 8. If the angle of attack is 0°, a lift force is already obtained because the flow of air is already deflected downwards by the asymmetrical shape of the wing. As the angle of attack increases, the lift coefficient increases until it reaches a maximum value. The rise is caused by the ever-increasing speed of the air at the top of the wing and consequently lower pressure opposite the bottom of the wing. The lift coefficient as a function of the angle of attack is shown in Figure 9.

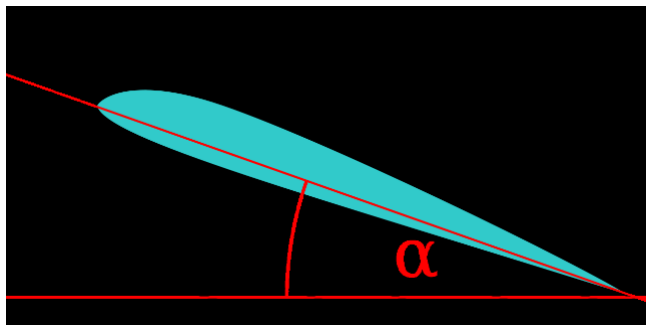


Figure 8: The angle of view

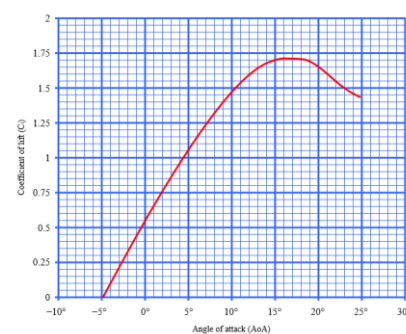


Figure 9: The lift coefficient as a function of the angle of attack

If the angle of attack is too large (usually around 15°), the airflow at the top of the wing can no longer follow and it will detach from it due to the low pressure. This creates air vortices on top of the wing, negating the upward force (see figure 10) [32]

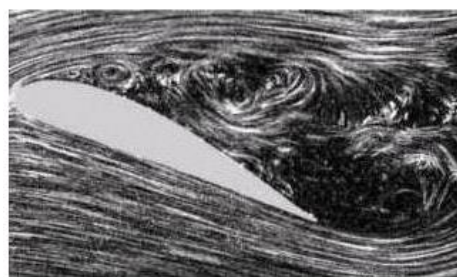


Figure 10: Flow on a wing at a small angle of attack (left) and at a large angle of attack (right)

1.5 Determination of the wind speed

A pitot tube is used to measure the wind speed in a wind tunnel. This is a simple measuring device consisting of a simple metal tube in which a few holes are drilled. The first hole is drilled in the front of the tube so that this hole is parallel to the airflow through the wind tunnel. The second and third holes are drilled perpendicular to this in such a way that they are perpendicular to the airflow in the wind tunnel. These holes allow air to enter the pitot tube and make it possible to measure a pressure difference between the air entering the front of the pitot tube and on both sides.

The shafts in the pitot tube perpendicular to the air flow only experience a static pressure (the atmospheric pressure). However, the shaft connected to the hole in the front of the pitot tube experiences both the static atmospheric pressure and an additional dynamic pressure due to the air velocity. The pressure difference that arises between the two shafts can easily be measured by, for example, connecting them on both sides of a tube filled with liquid and measuring the liquid in the U-tube (principle of connected vessels). A schematic representation of the pitot tube is shown in figure 11.

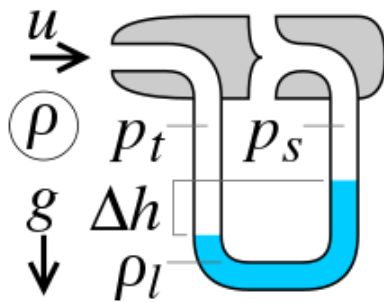


Figure 9: The pitot tube

The difference of the liquid level can later be entered into the Bernoulli equation to measure the air speed.

$$= +$$

$$2 = \frac{2 * (-)}{\rho_h}$$

Whereby:

- :total pressure
- :static pressure (atmospheric pressure)
- :dynamic pressure (pressure due to air speed in wind tunnel)
- :airspeed in wind tunnel
- ρ_h : density of the air

However, an accurate airspeed measurement using a pitot tube requires a sufficiently large airspeed. At very low airspeeds, the errors made on the measurements will become very large [29].

1.6 Wind tunnel

1.6.1 Definition and principle

A wind tunnel is a useful device for investigating different types of air currents. In a wind tunnel one can thus study the aerodynamic properties of an object. By placing an object in the wind tunnel, you can see the effect of the air on the object and of the object on the airflow. In this way, the object can be adjusted so that it behaves ideally in the air stream.

A wind tunnel, as shown in figure 12, always consists of a funnel in which the air is sucked in and contracted, a straight test section in which the object is placed, and a wider section 'the diffuser' that, through the fans (propellers) present, pushes the air into the tunnel sucks.

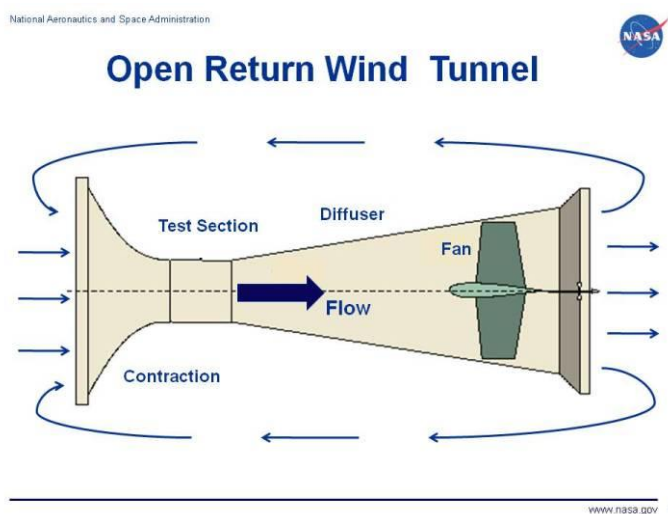


Figure 10: Sketch of a wind tunnel [27]

The principle of a wind tunnel is therefore quite simple. The propellers in the rear diffuser rotate to create an airflow in front of the opening of the wind tunnel, in the direction of the wind tunnel. The flow that is sucked in like this is turbulent in nature. This is solved by making a specific funnel structure at the beginning of the wind tunnel in which a honeycomb is present (see below). This reduces the average surface area and thus increases the speed of the air. Then we come to the test section, the place where the experiments are carried out. After the test section, the average surface area increases again and there is room for fans.

An advantage of using wind tunnels is that experiments can be conducted in a controlled environment, as opposed to exposure to the outside environment. A disadvantage is that scale models often have to be used, since a full-size object is often too large for many wind tunnels [31].

1.6.2 Types of wind tunnels

There are two types of wind tunnels, the open and the closed wind tunnels. Each has its advantages. It is up to us to weigh these against each other. An open wind tunnel is a wind tunnel that does not recirculate the air. The wind tunnel sucks air into the room longest at the front. So passes

the air passes through all parts of a wind tunnel and exits the chamber again through the back [10]. The major advantages of an open wind tunnel are that it is simple and more economical to build than a closed wind tunnel. The extra effort and cost are avoided as there are fewer ducts to design and build. The air flow visualization is also easier (smoke can enter longer for easier) and the air temperature rises less quickly. No air purification is required and smoke congestion is avoided. A sketch of an open wind tunnel is shown in Figure 13.

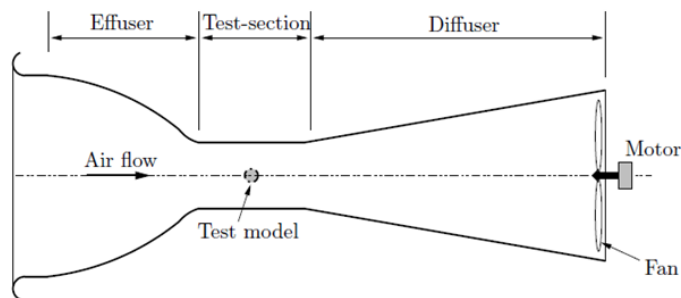


Figure 11: Open wind tunnel

A closed wind tunnel reuses the same air again. Once driven by the propeller, the air passes through a number of corners, then through the funnel with screens and honeycomb structure. Finally through the test section and the diffuser. In terms of construction, it looks almost the same as an open wind tunnel, with the only visible difference being that the sky follows the same path each time. This entails a number of advantages [5]. Less energy has to be used to obtain a certain air speed and the external factors in the room where the wind tunnel is located (air displacements or dust) have no influence on the air flow. In a closed wind tunnel, the air temperature rises faster. That is why a closed wind tunnel requires an air cooling system, which adds an additional complexity and cost to building it. [10, 5] A sketch of a closed wind tunnel is shown in Figure 14.

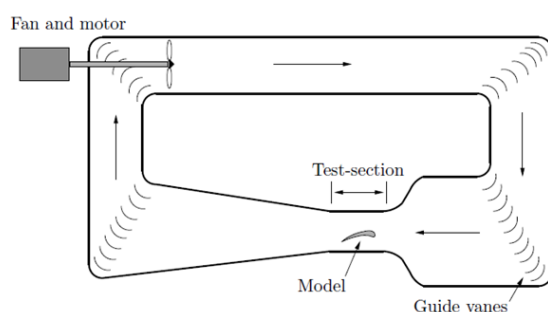


Figure 12: closed wind tunnel

1.6.3 Purpose of the project

The goal of this project is that we are able to design and build a wind tunnel ourselves that can generate laminar flow, so that we can perform experiments with results that correspond to those of industrial wind tunnels. In the experimental part of the project we want to find an answer to the following research question: Are we in

able to build a wind tunnel in which we can generate laminar flow, which we can then use to perform aerodynamic experiments? To answer this question, we have to divide our main research question into sub-questions:

1. What do you need to build a wind tunnel?
2. How do you generate laminar flow?
3. How can I visualize laminar flow?
4. How do you measure airspeed?
5. What is the airspeed in the wind tunnel
6. What is the best angle of attack to create lift on a wing?

2 Materials and Methods

2.1 Requirements and components of an open wind tunnel

To build a functional open wind tunnel that creates laminar flow, the components must meet important requirements. An open wind tunnel consists of 6 major parts: the honeycomb, screens, funnel, test section, diffuser and fans.

To obtain a laminar airflow, 1 honeycomb and 2 screens will be used and a contraction ratio of 5.09:1 will be used. [18]. A contraction ratio is the ratio of the area between the inlet of the wind tunnel and the outlet of the test section.

2.1.1 Honeycomb

The airflow is made laminar via a honeycomb structure. The cross section of the individual cells of our honeycomb is round. Normally a honeycomb is always hexagonal, but in this document we will always speak of a 'honeycomb'. A honeycomb is a collection of channels that point in the same direction as the airflow. This minimizes cross-flows of the air stream as it enters the wind tunnel.

An optimal ratio of diameter to length of each cell in the honeycomb is 1:10. [36] However, this is what we also strive for. Others claim that a ratio of 1:6 is enough [28]. Of course it doesn't hurt if the cells are longer. We have chosen straws as material for the cells, which are cheap and have an optimal diameter of 0.6 cm. The usable part of the straws (not counting the pliable side) is 18.0 cm long. This 18.0 cm is always cut into 3 parts of 6.0 cm. Thus, the desired ratio of 1:10 has been achieved. Then the shorter straws are placed next to each other and glued together. It is estimated that 2100 straws were used for the honeycomb, so almost 6400 small, individual straws stacked on top of each other and next to each other.

To keep the honeycomb together, 4 panels of 3mm thick MDF are mounted in a square around the honeycomb. The honeycomb is then placed in the beginning of the funnel. In this part of the wind tunnel there is a low wind speed and high pressures, so that the air flow is turbulent.

Since the pressure loss is proportional to the mean speed of the fluid flow, the manipulators are generally installed in the low-speed portion of the wind tunnel. [SCHEIMAN, 1981, page 1]. Translation: Since the pressure drop is proportional to the speed of the liquid flow, the manipulators (in our case the honeycomb and the screens) are generally installed in the low-speed part of the wind tunnel.

Images of making the honeycomb structure are shown in Figure 15 and 16.



Figure 15: structure of the honeycomb



Figure 16: The finished honeycomb

2.1.2 Screens

In addition to the honeycomb structure, 'the screens' are also an important part of the funnel to achieve laminar flow. The screens we have chosen are made of mosquito net with a hexagonal shape as shown in figures 17 and 18.

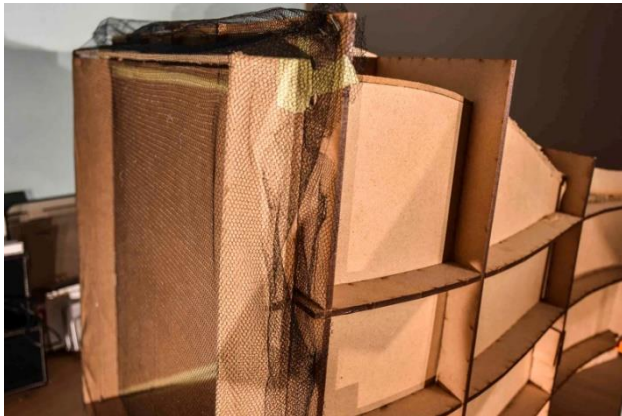


Figure 17: The funnel with the screens mounted

The screens will ensure that the axial turbulence due to the pressure difference in the cross-section decreases, while the honeycomb will mainly reduce the lateral turbulence [35]. So both constructions are necessary.

To calculate the opening of the mosquito net, we use the following formula [23]:

$$\frac{2 \times 100}{2} = \%$$

With the opening size S of 2.0 mm and an intermediate distance C of 2.5 mm (these measurements were made with a digital caliper and are shown in figure 18) we obtain a percentage of 64%.

$$\frac{2.0}{2.5} \times 100 = 64\%$$

The screen used in the funnel is woven nylon thread and therefore has an opening of 64% (with our measurements).

These openings should not match the openings of the honeycomb. We use two screens in the wind tunnel, the first at 45mm from the honeycomb and the second at 45mm from the first screen. Placing two screens is sufficient for us to achieve the level of turbulence that we want to achieve. [38]

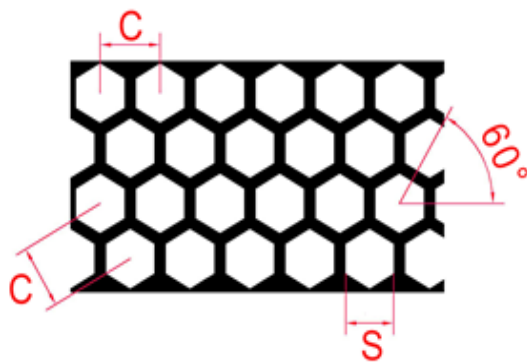


Figure 18: The honeycomb structure of the mosquito net

2.1.3 The Funnel

The funnel has a specific curved shape.

The shape of this bend is made according to a number of conditions:

1. Contraction ratio of 5.09:1. [18]
2. The slats must be able to be cut on a plate that is a maximum of 60.0 cm long and 30.0 cm high (this is the maximum size that fits in the laser cutters).
3. Minimal flow separation (flow separates from a surface).

To make the funnel, 3mm MDF was used for both the skeleton structure and the inside. The skeletal structure was cut out with a laser cutter in the Fablab Leuven at the Arenberg campus III.

To determine the shape of the funnel we use a polynomial of the fifth order (the highest power in 5), proposed by Bell & Metha [30].

$$= (-10x^3 + 15x^4 - 6x^5)(x - y) +$$

Whereby, $x = \frac{r}{R}$ and $y = \frac{z}{L}$

The variables to be determined by us are:

1. L , length of the contraction: We chose L 58.0 cm, as the maximum length of a slat is 60.0 cm and we wanted to leave some margin to make the cutting process easier.
2. H_{you} , (height of contraction outlet measured from midline). In the original design we have H_{you} equal to 10.0 cm, but due to inaccurate bending this has become 9.5 cm.
3. For H_i , (height of the contraction inlet measured from the midline) we chose 22.56 cm.

To achieve a contraction ratio of 5.09:1 we must therefore make A_i 5.09 times larger than A_u and the height of the inlet will therefore be 22.56 cm as worked out in the following calculations:

$$= \quad : \quad = (\times 2)^2 = 400 \quad 2$$

$$= \quad : \quad = \times 5.09 = 2036 \quad 2$$

Now we need this surface calculate back to .

$$= (\times 2)^2$$

$$= \frac{\sqrt{\quad}}{2}$$

$$= 22.56$$

If we fill all these values into the formula, the graph will look as shown in figure 19.

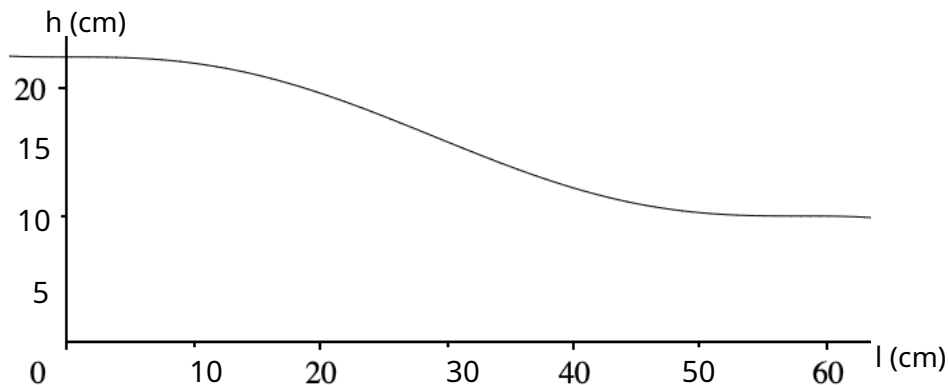


Figure 19: The bending of the funnel we use, the useful domain for us is: $l \in [0.58]$

In this way the shape of the funnel is fixed. The funnel consists of two parts: the skeletal structure and the inner walls. The skeletal structure consists of 3 consecutive square frames. Three slats with a curved shape are attached on all sides in the opening of the frames. So twelve slats in total. This forms the sturdiness of the funnel and the basis for the inner walls. The skeleton structure is shown in figure 20. In this structure, four sheets of 3mm MDF are then bent one by one on each side and glued. To make the plates flexible, they were first moistened with warm water. After this they are placed in the structure and with weights (spread over the surface).

bent to the correct shape until the wood has dried. Now the wood is glued to the structure. This happens four times, once for each side. The placement of the inner walls and the use of weights is shown in figure 21. All MDF panels were cut in the FabLab of the Catholic University of Leuven.



Figure 20: The skeletal structure



Figure 21: The inner walls that are folded by weights

The finished funnel is shown in Figure 22.



Figure 22: The finished funnel

2.1.4 The test section

The testing section is what it's all about. This is where the highest air speed is reached and the tests are therefore also carried out. We aimed for a test section of 20 x 20 cm. Because we had to make adjustments, our test section now measures 19.0 x 18.0 cm and is 58.0 cm long. The length of the wind tunnel is limited by the maximum length of the MDF panels, plus a large cutting margin. The walls are made of 9mm MDF, cut out in the Fablab. We replaced the MDF in the first half, the front and top of the test section

through 2mm plexiglass. This allows us, as with many wind tunnels of this size, to look inside and visualize airflow. We also have a 10 mm hole in the bottom in the middle of the visible part of the test section. This allows test equipment to be used and aircraft wings to be directly connected to an external balance. An image of the test section is given in Figure 23.

To maintain accurate results, the test item in the test section should be allowed to flow freely not prevent too much. The rule here is: The cross-sectional area of the test article may not exceed 10% of the cross-sectional area of the test section [28].



Figure 23: The finished test section

2.1.5 diffuser

To achieve higher speeds in the test section itself, we placed a diffuser between the test section and the fans. The diffuser also has a funnel shape made of 3 mm MDF plates glued together. Due to the funnel shape, the test section has a smaller diameter than the diffuser and the air pressure in the test section is lower than the air pressure in the diffuser, see Bernoulli's law. As a result, the speed in the test section is higher than the speed in the diffuser. The advantage of this shape is that we can run the fans at a lower speed (rpm), and therefore put less stress on the entire electronic circuit. An image of the diffuser is shown in Figure 24.

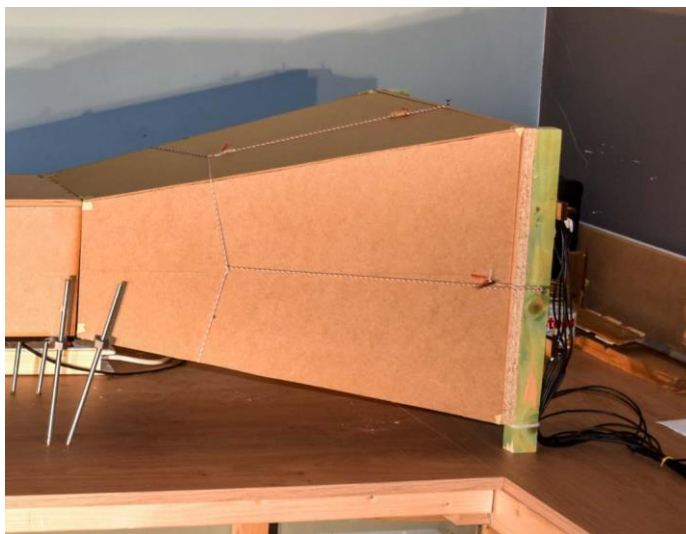


Figure 24: The diffuser

2.1.6 Fans

We opted for four fans for an even distribution of the air intake. The 4 fans each consist of a propeller driven by a motor. A schematic representation of the electronic control of the motors is shown in figure 25 and a photograph of all parts of the fans is shown in figure 26.

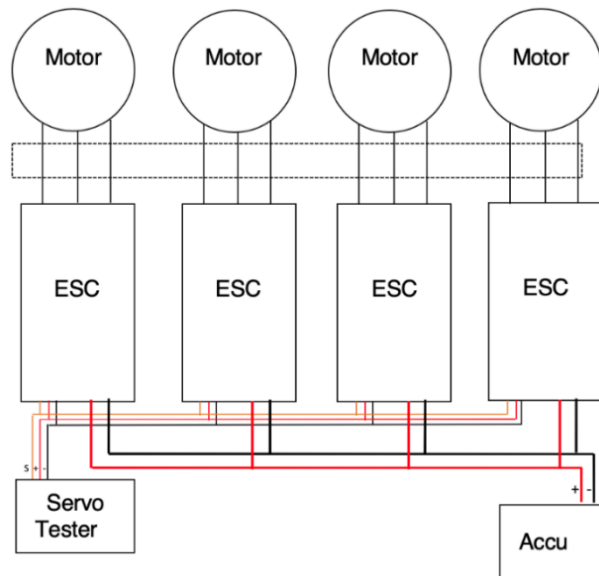


Figure 25. Schematic overview of the electronic control of the motors



Figure 26: All parts of the fans.

The fans are made up of a number of different parts with specific requirements:

1. We chose 3 blade propellers. For example, the air discharge is better distributed over the surface of all fans together. The diameter of these propellers is chosen in function of the size of the diffuser opening.
2. As a motor we use four brushless motors of the type "Racerstar BR2212 1400KV 2-4S Brushless Motor For RC-models". (see table 1)
3. An electronic speed controller, also called ESC (Electronic Speed Controller), is placed on each motor. This ensures that the revolutions per minute (rpm) remain constant.
4. The wiring used between the motors and the ESCs are 1.5mm (diameter) with a flexible PVC housing
5. The battery used to power the motors is a LiPo (lithium ion polymer battery) 6000mAh, 7.4V, 60C.
6. A servo tester is required to ensure proper operation of fans. They give a signal to the ESC so that the ESCs know how much power to give from the battery to the motors.

Table 1 shows the specifications at voltage 11.1 V of the propellers we purchased from 'banggood.com website'. However, we have used a voltage of 7.4 V.

Fashion model	Tension (V)	Amperage (A)	Pull (g)	Assets (W)	efficiency (g/w)
BR2212 1400KV	11.1	19.0	910	210	4.3

Table 1: Engine specifications

In table 2 you will find a summary of the components of the fans.

Element	Description	Specifications
1.	Propeller	Diameter: 17.8 cm, 3 leaf, plastic.
2.	engine	input voltage = 7.4-14.8V, 210W.
3.	Wires	Diameter: 1.5 mm, flexible PVC.
4.	ESC	=30A.
5.	Battery	Li-ion polymer battery, 6000mAh, = 360A, U = 7.4V (2 cell). Input: U = 4.2-6.0V.
6.	servo tester	

Table 2: Parts of the fans

The propellers are placed in a laminated OSB board of 430 x430 mm and 15 mm thick with 4 holes cut out of 185.0 mm in diameter. These holes were cut with a milling machine according to the pattern shown in Figure 27. The fans were then soldered together.

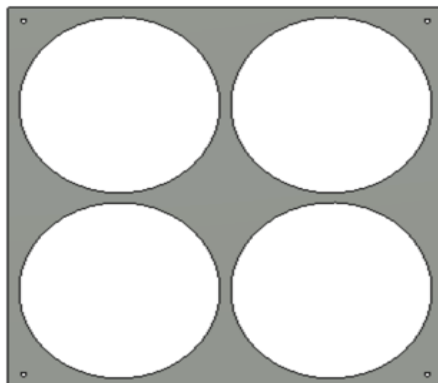


Figure 27: The pattern in which the holes are cut.

This plate, in which the propellers are mounted, is connected to the diffuser with a tensioned rope as shown in figure 24.

In summary, the requirements of the different sections of a wind tunnel are shown in Table 3. [18]

Element	Description	
1.	Honeycomb	A = 43.5cm x 43.5cm, 0.6 x 6.0cm
2.	Screens	64% open, 138M
3.	Funnel	CV = 5.09
4.	Test section	A = 19.0cm x 18.0cm, L=58.0cm
5.	diffuser	$\alpha = -11^\circ$
6.	Fan (motors + propellers + electrical circuit)	4x 210W max, 17.8 cm 3 leaf

Table 3: Requirements of the components of a wind tunnel

2.2 Assembly of the wind tunnel

The funnel, the test section and the diffuser with the propellers are then put together and to support the whole structure we used a system with adjustable uprights. These are made from a threaded rod and a bolt. The bolt is held by a 3D printed part and attached to the different parts of the wind tunnel. The threaded rod was attached below. It adjusts in height by turning the threaded rod. A photograph of the wind tunnel with the legs is shown in Figure 28.



Figure 28: The legs under the wind tunnel

2.3 Materials for the construction of the wind tunnel

- For the design we used a 3D software program 'Fusion 360 (educational license)'
- We used 3mm MDF (Brico) for the funnel wall, the diffuser, the frame of the honeycomb and the intermediate pieces for the mosquito net. These panels are each cut with a pendulum saw. MDF is a soft and light wood that is easy to work with.
- For the funnel skeleton structure we also used 3mm MDF from the FabLab in Leuven. We also cut these in the FabLab with their laser cutters.
- 9mm MDF was used for part of the test section. This way the sides hang better together, without us having to use external support.
- The transparent part of the test section is made of 2mm plexiglass. This was also purchased from the FabLab and cut there with their laser cutters as well.
- The propeller structure is cut out of a laminated OSB board measuring 430 x 430 mm and 15 mm thick.
- The honeycomb structure is mainly made of plastic straws. These are glued together with craft glue and a 3mm MDF frame is placed around all the straws.
- The mosquito net is made of nylon thread woven in such a way that a hexagonal mosquito net is created.

2.3.1 Additional production machines

Various machines and tools are used to make the above mentioned parts. Below is some more technical information.

1. The laser cutter we used is in the fablab of the brand Trotec Speedy 100R with the following specifications (610 x 305 mm working space, 132 mm maximum material thickness, 10-120 Watt laser)
2. The milling machine used is self-designed and made with inspiration taken from the DIY 3D Printed Dremel CNC" by Nikodem Bartnik. [33]. This milling machine had the following specifications
 - 470 x 440 mm working space
 - 80 mm material thickness (limited to drill head length).
 - 17mm Flat Head Double Flute Spiral Chuck.
 - Multi-tool: *Dremel 4000*.
3. The 3D printer (Prusa i3 MK2/S) was used to print the airplane wing and the bolts of the uprights.
 - Cartesian printer
 - 250 x 210 x 200mm print volume (XYZ).
 - 1.75mm PLA plastic.
4. The multi-tool (Dremel 4000, 5000-35000 rpm and 175W): This is used to cut small things and edit the details. For example, a bit of material protruded somewhere near the funnel and we were able to quickly correct this with the multi-tool. This is also mounted on the milling machine to cut out the propeller structure.
5. The Martin magnum 800 was used as a smoke machine.

3 Practical trial

3.1 Wind tunnel design

When designing the wind tunnel, we went through two different versions. The first version was made before we visited BikeValley. During our visit we learned from Harm Ubens that we had to take into account certain elements that were important for the design of the wind tunnel [38]:

1. Harm Ubbens from BikeValley told us that the angles between the funnel and the test section should not be too sharp. If the angle is too sharp, the flow will separate from the wall, generating large pressure differences in the test section.
 2. To create a laminar flow, the air speed should be as low as possible. If this happens just before the test section, the air speed will be higher than just before the diffuser. The lower the velocity in the honeycomb structure, the more laminar the flow.
 3. It is recommended to use 4 less powerful fans compared to using one fan that would suck in all the air. In addition, the diffuser must have a funnel shape so that the fans have to run less hard.
 4. The presence of screens is essential to reduce axial turbulence.
- [30]

This is how we came to the development of a second and final version. We avoided sharp corners, installed screens and placed the honeycomb structure in front of the funnel. We also used several fans. The complete wind tunnel setup is shown in Figure 29

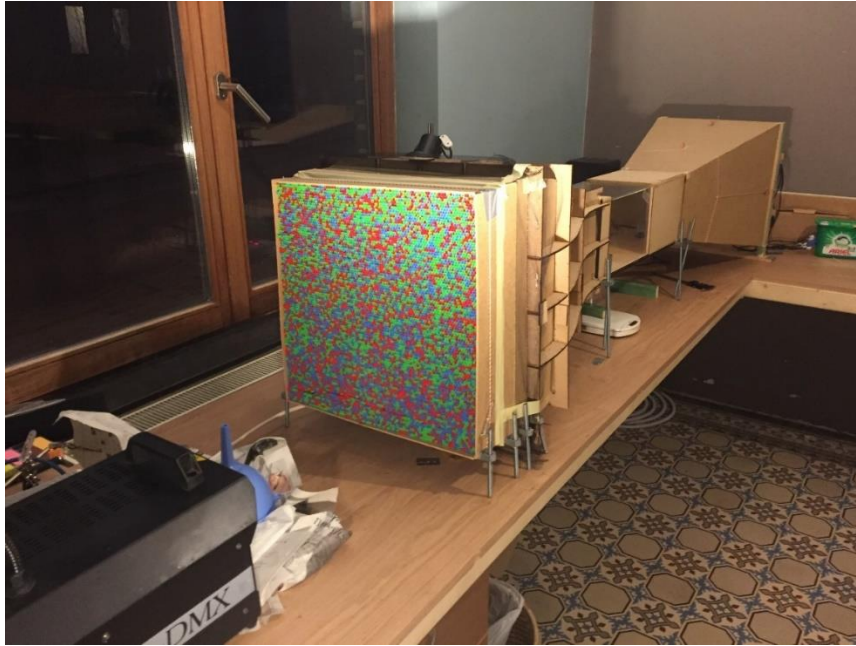


Figure 29: The general setup of the wind tunnel

3.2 Making laminar flow visible

Once the wind tunnel was assembled, we could start our experimental part. Important here is that we were able to visualize the air flow that we generated in the wind tunnel. For this a smoke machine was used that was placed just before the funnel as shown in figure 29. At maximum speed of the fans we could demonstrate laminar flow as shown in figures 30, 31 and 32. During this process different shapes were used in the test section. placed.



Figure 30: flow at a bus



Figure 31: Current at an old-timer



Figure 32: Current in a racing car

3.3 Determining the airspeed

3.3.1 Parts of the test set-up when determining the airspeed

The following materials were used to determine the air speed:

- pitot tube (PT60 tube air speed meter sensor kit differential for pixhawk APM PX4 flight)
- wooden beam to attach pitot tube with bolts
- gin with 40 V% alcohol
- 2 flexible transparent hoses
- U-shaped iron staples
- Wooden board with mm paper stuck on it

To determine the air speed, the pitot tube was screwed onto a wooden beam and connected to flexible hoses filled with gin (40 V% alcohol). The hoses are attached in a U-shape with iron staples to a plate on which mm paper is pasted. The fans are set in different speed positions and the height difference of the liquid is read through the mm paper.

An image of the complete setup is shown in Figure 33.

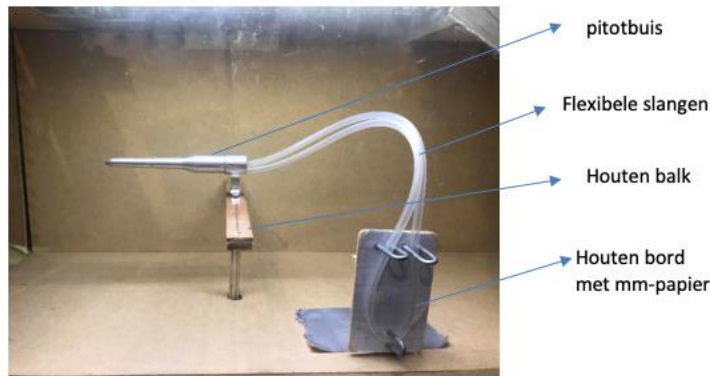


Figure 33: Illustration of the pitot tube setup in the test section

We had to use a 40% alcohol solution to measure the air speed because measurements could not be made with water. The cohesion between water and the hose was in fact too great to cause a displacement of the water column.

The following formula was used to calculate the speed:

$$v = \sqrt{\frac{2 \cdot \Delta h \cdot \rho_{\text{liquid}} \cdot g}{\rho_{\text{air}}}}$$

whereby:

- h=height difference
- ρ_{liquid} = density of liquid (930 kg/m³) g= gravitational acceleration (9.81 m/s²)
- ρ_{air} = density of air at 15°C (1.225 kg/m³)

To measure the speed at different places in the test section, the pitot tube is also moved to different points in the cross-section of the test section.

3.3.2 Measurement of the air speed at the maximum position of the fan

The speed of the air was determined at the highest setting of the fan and at various locations in the test section of the wind tunnel.

As shown schematically in Table 4, the wind tunnel was divided imaginatively into nine equal parts. In each case, the pitot tube was placed in the middle of a part of this imaginary section and a measurement was taken at each location. The results of these measurements are shown in Table 5.

Height/ width	Left	Middle	Right
Upstairs	9	3	6
Middle	8	2	5
below	7	1	4

Table 4: Placement of the pitot tube in the test section

At the nine different places in the measurement section, the measured airspeed was very analogous. The airspeed was between 33 and 35 km/h. From this we can conclude that the airflow is homogeneously distributed in the cross-section of the test section.

Position	Δh (mm)	v (m/s)	v (in km/h)
1	5.5	9.1	33
2	5.6	9.1	33
3	5.2	8.8	32
4	6.1	9.5	33
5	6.0	9.5	34
6	6.1	9.5	34
7	6.2	9.6	35
8	5.6	9.1	33
9	5.8	9.3	34
Average		9.3	33

Table 5: Determination of homogeneity at maximum fan speed

3.3.3 Measurement of airspeed at predetermined settings

Subsequently, the air speed at fixed fan settings was measured in the center of the wind tunnel (position 2 in table 4). The results are shown in Table 6. We can demonstrate a linear relationship between air speed and fan speed as shown in Figure 34.

fan-stand	Δh (in mm)	v (in m/s)	v (in km/h)
1	0.0	0.0	0.0
2	0.2	1.7	6.2
3	2.0	5.5	20
4	4.0	7.7	28
5	5.7	9.2	33

Table 6: Determining the air speed at different fan speeds

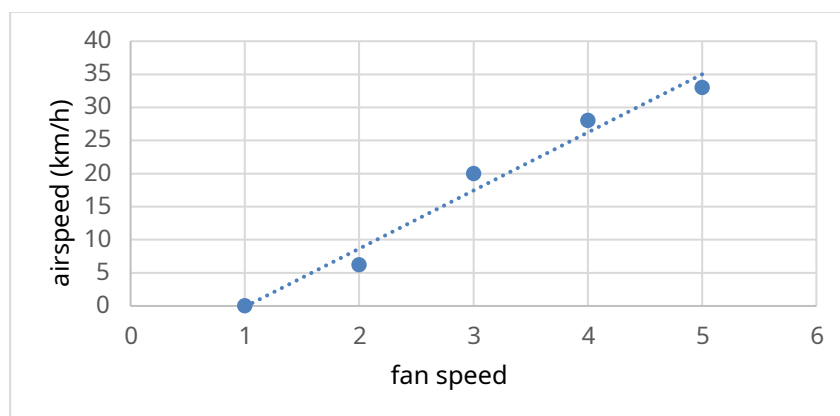


Figure 14: Relation of air speed to fan speed

3.4 Determination of the lift of a wing at different angles of attack

3.4.1 Method of measuring lift on a wing

The following materials were used to demonstrate the lift of a wing:

- Kitchen scale (Brabantia max 3kg/1g)
- Wooden block with opening
- Metal rod with pliable tip
- 3D printed airplane wing (NACA 4412) (airfoiltools)
- Opening in the bottom of the wind tunnel test section 10mm

To measure the lift of the wing, the 3D printed wing is placed on the tip of a metal bar. The metal rod then goes into the opening of the bottom of the test section. A kitchen scale is placed under the test section of the wind tunnel. A hole is drilled in a wooden block and placed on the scale. The balance is tared to zero. The metal rod with the wing is placed in the drilled hole. The initial mass of the wing is read. Then the fans are started at a specific speed. The mass is now read again. This is repeated at different angles of attack of the wing. The mass difference between the initial value and the final value is then converted into a force ($F = -mg$).

To prevent the wooden block from coming loose from the scale (and thus incorrect values being measured), it was attached to the scale with adhesive tape at high air velocities.

An image of the wing setup in the test section is shown in Figure 35

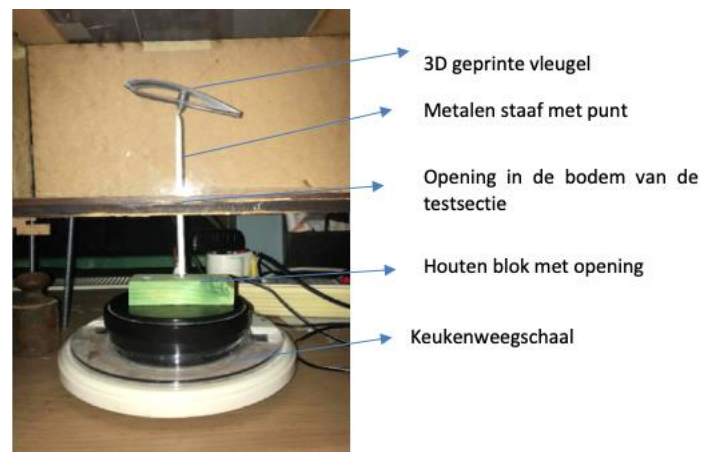


Figure 35: The arrangement of the wing in the test section

The wing was always placed at a certain angle of attack. The angle of attack was measured as shown in figure 36. A photograph was taken of the wing at a certain angle and the angle to the ground plane was determined with a protractor.

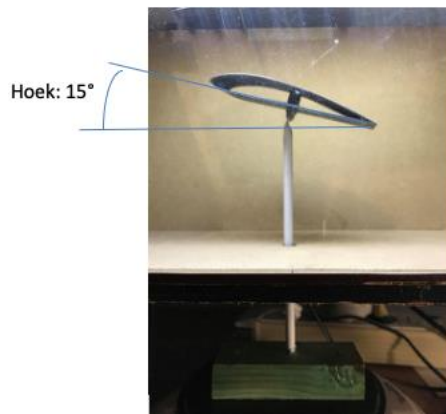


Figure 36: Measurement of the angle of attack of the wing

3.4.2 Determination of the lift force and lift coefficient as a function of the angle of attack

At the maximum airspeed of 33 km/h, the lift on the wing was determined at angles of attack in the range of 0° and 60°. The results are shown in Table 7

angle of attack (°)	m (g)	-m (g)	F lift (mN)	C _{elevator}
- 60	74	- 12	- 12.10	- 0.52
- 50	79	- 8	- 78	- 0.35
- 40	80	- 16	- 16.10	- 0.69
- 30	78	- 17	- 17.10	- 0.74
- 20	69	- 8	- 78	- 0.35
- 10	69	- 6	- 59	- 0.26
0	49	2	20	0.09
10	46	9	88	0.39
20	33	20	20.10	0.87
30	32	31	30.10	1.3
40	34	30	30.10	1.3
50	30	25	25.10	1.1
60	45	10	98	0.43

Table 7: Determination of lift at different angles of attack

In figure 37 the lift force was plotted as a function of different angles of attack (blue curve). We find that it increases to a critical angle of 30° after which the lift force drops again. The critical angle of attack in our wing is higher than that described in the literature. It is described that a wing loses its lift at an angle of 15° to 20° [11]. So in our experiments this is 10° higher. This variation may be explained by a different way of measuring the angle of attack. At negative angles we notice that the mass of the wing increases and that the wing is pushed against the bottom.

From the experiments, the lift coefficient can also be determined by using the formula of Bernoulli's law:

$$C_L = \frac{2 \cdot L}{\rho \cdot V^2 \cdot S}$$

of:

-the density of air (1.225 kg/m³) v the
airspeed (9.3 m/s)

S the area of the wing (43 cm²= 43.10⁻⁴m²) c_Lthe lift
coefficient relative to the angle of attack -

Subsequently, the lift coefficient was also plotted as a function of the angle of attack in Figure 37 (red curve).

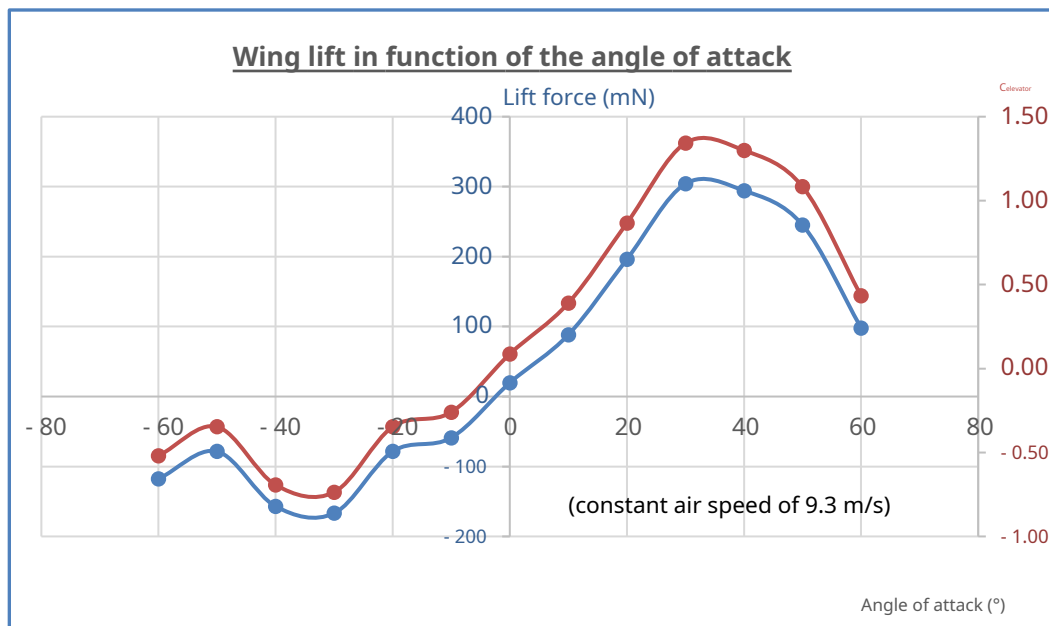


Figure 37: Wing lift as a function of the angle of attack

In terms of magnitude, the lift coefficients obtained correspond well with what is reported in the literature for a wing of this type (NACA 4412) (see figure 38) [20]

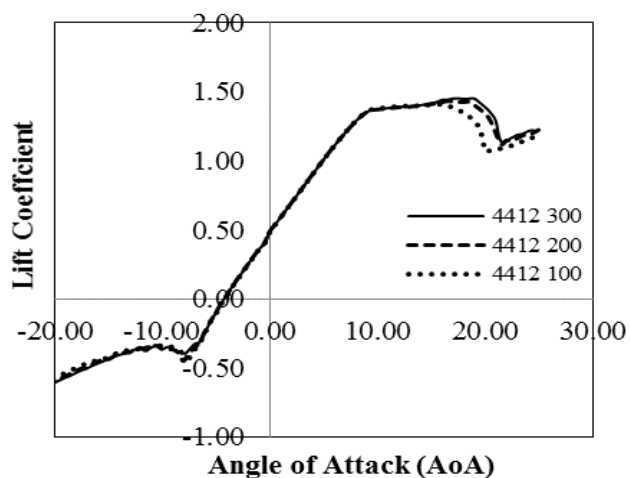


Figure 38: Calculated and experimental lift coefficient as a function of angle of attack [20]

3.4.3 Lift force and lift coefficient as a function of airspeed

At various airspeeds of Table 6, the lift force on the wing was determined experimentally at a constant angle of attack of 30°. In addition, the theoretical lift force was also calculated using the following formula:

$$F_{\text{lift}} = \frac{1}{2} \rho v^2 S C_L$$

Whereby::

-the density of air at 15°C (1.225 kg/m³) v the airspeed (m/s)

S the area of the wing (43.10⁻⁴m²)

C_L the lift coefficient relative to the angle of attack - of 30° is 1.3 (see table 7)

The experimental (-mg) and theoretical results are shown in Table 8 and plotted in Figure 39. For our wing, the experimental values are C_{elevator}= 1.34 at 30° angle of attack and the area of the wing is 43 cm².

v(m/s)	-m (g)	F elevator (mN) (exp)	F lift (mN) (theory)
0.00	0	0	0
1.7	2	20	11
5.5	24	24.10	11.10
7.7	29	28.10	21.10
9.2	36	35.10	30.10

Table 8: Determination of lift at different airspeeds.

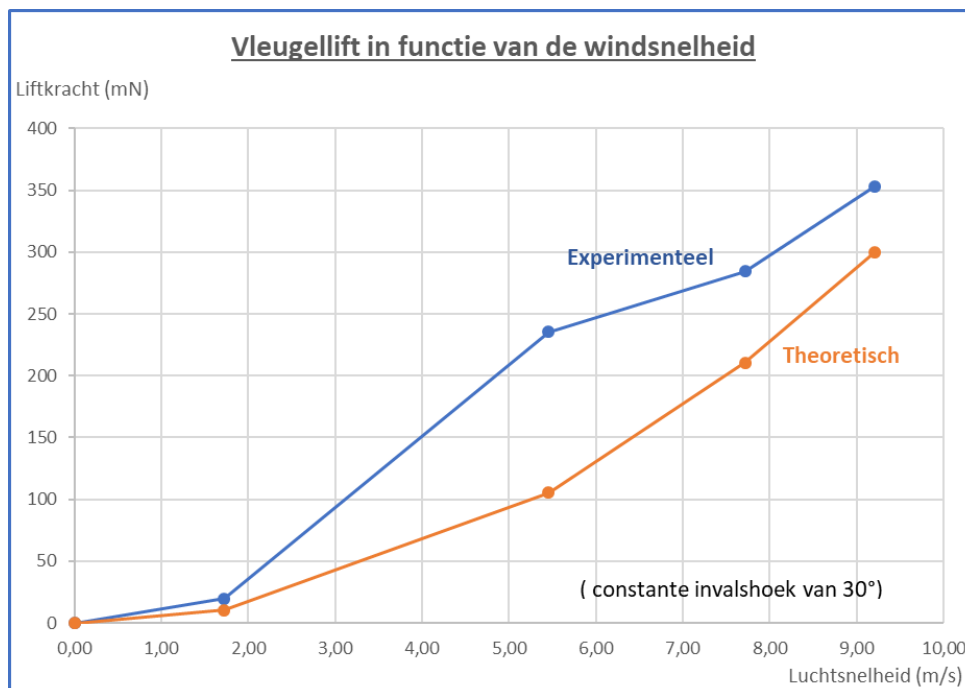


Figure 39: Wing lift as a function of wind speed

If we compare the theoretical curve, which shows a quadratic variation, with the experimental curve, we notice that the experimental curve shows a similar variation except for one deviating point at 5.5 m/s. The reason for this deviation may be due to an inaccurate measurement of the mass of the wing at that speed.

4 General decision

A wind tunnel is a device that allows a scientist to study the airflow on an object and the additional forces on the object. Originally, a wind tunnel was used to study the aerodynamic properties of an aircraft. Currently, a wind tunnel is used in many disciplines such as the automotive industry, architecture, sports, ...

In this research work, we built an open wind tunnel in which we were able to generate a laminar flow. A wind tunnel always consists of a funnel, a test section and a diffuser in which fans are present. To obtain laminar flow, the funnel into which the air is sucked must meet a number of conditions. There should be a honeycomb consisting of a lot of channels (in our case 6 cm straws) pointing in the same direction as the airflow. In addition, screens are also required to absorb the large pressure differences. These are made of nylon thread woven into a mosquito net. The highest air speed is reached in the test section and the experiments also take place there. Next there is a diffuser. This is also made in the form of a funnel in which 4 fans are placed.

We used a smoke machine to visualize the laminar flow. This smoke machine was placed in front of the funnel so that the smoke was sucked into the wind tunnel. We were able to visualize the air flow around a bus, an old-timer and a racing car. Different wind speeds were obtained via different positions of the fans, which we could measure via a pitot tube. A maximum wind speed of 33 km/h was measured. Subsequently, an aircraft wing of model NACA 4412 was printed using a 3D printer. This wing was used as a test wing to demonstrate lift on the wing. The lift force on a wing was determined at different angles of attack. For example, we were able to demonstrate that the lift force increases to a critical angle of 30° , after which the lift force drops again. This critical angle in our experiments is higher than the 15° angle that we could find in the literature. In addition, the lift coefficient was calculated at different angles of attack. These lift coefficients are in good agreement with the lift coefficients that we could find in the literature for this wing type. As a final experiment, we were able to demonstrate a quadratic relationship between wing lift and wind speed.

5 Literature list

- 1) ABUNAN, B., *XFoil predicted lift coefficient for NACA 4412 versus experimental data*, internet, (February 9, 2020), (https://www.researchgate.net/figure/XFoil-predicted-liftcoefficient-for-NACA-4412-versus-experimental-data_fig1_309731963).
- 2) AIRFOILTOOLS, NACA 4412 airfoil, internet, (nd), (<http://airfoiltools.com/airfoil/details?airfoil=naca4412-il>)
- 3) ANOINYEM, Life (force), internet , Wikipedia, January 29, 2020, ([https://en.wikipedia.org/wiki/Lift_\(force\)](https://en.wikipedia.org/wiki/Lift_(force)))
- 4) ANONYMOUS, *aerodynamics*, internet, Wikipedia, (November 21, 2019), (http://www.woordlijst.eu/betekenis_aerodynamic.htm).
- 5) ANONYMOUS, *Closed return wind tunnel*, web, (January 2020), (<https://www.grc.nasa.gov/www/k-12/airplane/tuncret.html>).
- 6) ANONYMOUS, *Coanda effect*, Internet, Wikipedia, December 21, 2019, (https://en.wikipedia.org/wiki/Coand%C4%83_effect) (Figure 5).
- 7) ANONYMOUS, *Daniel Bernoulli*, Internet, Wikipedia, (15 January 2020), (https://en.wikipedia.org/wiki/Daniel_Bernoulli).
- 8) ANONYMOUS, *The flow profile*, internet, (2020), (<https://www.flowmeters.nl/relevantezaken/flowprofile>).
- 9) ANONYMOUS, Laminar Flow, Internet, *Wikipedia*, November 12, 2019 (https://nl.wikipedia.org/wiki/Laminaire_stroom).
- 10) ANONYMOUS, *open-return wind tunnel*, internet, (January 2020), (<https://www.grc.nasa.gov/www/k-12/airplane/tunoret.html>).
- 11) ANONYMOUS, Overtrek, Internet, Wikipedia, September 9, 2019, (<https://en.wikipedia.org/wiki/Overtrek>)
- 12) ANONYMOUS, Propeller, Internet, *Wikipedia*, 12 December 2019, (<https://nl.wikipedia.org/wiki/Propeller>).
- 13) ANONYMOUS, Jet Engine, Internet, *Wikipedia*, February 2, 2020, (<https://nl.wikipedia.org/wiki/Straalmotor>).
- 14) ANONYMOUS, Turbulent Flow, Internet, *Wikipedia*, 12 November 2019, (https://nl.wikipedia.org/wiki/Turbulent_stroom).
- 15) ANONYMOUS, Wing (Airplane), Internet, *Wikipedia*, 11 May 2019, ([https://nl.wikipedia.org/wiki/Vleugel_\(aircraft\)](https://nl.wikipedia.org/wiki/Vleugel_(aircraft)))
- 16) ANONYMOUS, *Bernoulli's law*, unpublished dissertation, 17 pages.
- 17) ANONYMOUS, *Who invented the wind tunnel*, web, (February 6, 2020). https://www.centennialofflight.net/wbh/wr_experience/tunnel/testing/ED.htm).
- 18) CELIS, B. and UBBENS, H., *Design and construction of an open-circuit wind tunnel with specific measurement equipment for cycling*, unpublished dissertation, Flanders Bike Valley, Paal-Beringen, 2016, 5 pages.
- 19) CONVENT, MARC-ANTOINE, Flying, art or physics?, internet, (unknown), (<http://users.telenet.be/aerodynamica/>).
- 20) Danao, L., A., Abuan, E., Howell, R., Design analysis of a horizontal axis tidal turbine, Conference: Asian Wave and Tidal Conference, 2016
- 21) DREAMTIME, Airplane wing, internet, (nd), (<https://www.dreamstime.com/stock-illustration-airplane-wing-cross-section-body-lifting-forces-image48039697>)
- 22) EDITOR AEROLAB, *Closed Circuit Wind Tunnels*, internet, (unknown), (<https://www.aerolab.com/products/closed-circuit-wind-tunnels/>).

- 23) AEROLAB EDITOR, *Open Circuit Wind Tunnels*, Internet, (unknown), (<https://www.aerolab.com/products/open-circuit-wind-tunnels/>).
- 24) EDITOR BOEGER, *How to Calculate Perforated Metal Sheet Open Area* Internet, (unknown), (<https://www.perforated-sheet.com/calculation/how-to-calculate-openarea.html>).
- 25) PHOTO, *The Reynolds number*, internet, (September 10, 2010), (<https://www.modelbouwforum.nl/threads/het-getal-van-reynolds.118439/>).
- 26) HALL, N, NASA Incorrect Theory, Internet, (April 05, 2018), (<https://www.grc.nasa.gov/www/k-12/airplane/wrong1.html>)
- 27) HALL, N, NASA Open Return Wind Tunnel , Web, (May 05 2015) , (<https://www.grc.nasa.gov/www/k-12/airplane/tunoret.html>)
- 28) HERNANDEZ, G. and LOPEZ, M., *Design Methodology for a Quick and Low-Cost Wind Tunnel*, unpublished dissertation, 2013, 22 pp.
- 29) KEES, *Pitot tube aeronautical and marine*, internet, November 19, 2018, (<http://zienenweten.blogspot.com/2018/11/pitot-buis-lucht-en-scheepvaart.html>).
- 30) LAKSHMAN, R. and BASAK, R., Analysis of transformed fifth order polynomial curve for the contraction of wind tunnel by using OpenFOAM, unpublished dissertation, National Institute of Technology Sikkim Ravangla Mechanical Engineering, South Sikkim, 2018, 6pp.
- 31) Lindgren, B; Johansson, AV, Evaluation of the flow quality in the MTL Wind-Tunnel, 2002, Technical reports from royal institute of technology department of mechanics, Stockholm, Sweden.
- 32) Lindner, B., *The laws of flight*, internet, (unknown), (<https://www.natuurkunde.nl/artikelen/1762/de-wetten-van-de-vliegkunst>).
- 33) Nikus, *DIY 3D Printed Dremel CNC*, internet, (unknown), (<https://www.instructables.com/id/DIY-3D-Printed-Dremel-CNC/>).
- 34) NTR, (reg.), Who was Daniel Bernoulli, video, Schooltv, Netherlands, 2014.
- 35) Santos, R., M., an Mesquita, A., L. Development of an open-circuit low-speed wind tunnel, 2015 23rd ABCM International Congress of Mechanical Engineering, December 6-11, Rio de Janeiro
- 36) SCHEIMAN, J., *Considerations for the Installation of Honeycomb and Screens To Reduce Wind-Tunnel turbulence*, unpublished dissertation, Langley Research Center NASA Scientific and Technical Information Branch, Hampton, 1981, 49p.
- 37) THE EDITORS OF ENCYCLOPAEDIA BRITANNICA, *Osborne Reynolds*, (August 19, 2019), (<https://www.britannica.com/biography/Osborne-Reynolds>).
- 38) UBBENS, H, (Engineer Bike Valley), inform, Bike Valley, Beringen, October 2, 2019.
- 39) VAN DER VEEN, R. and STEL, B., *How does an airplane fly* Internet, (unknown), (<https://www.sciencespace.nl/technologie/articles/3900/hoe-vliegt-een-vliegt>).

6 List of figures

Figure 1: Replica of the first wind tunnel	9
Figure 2: Forces on an aircraft	11
Figure 3: Turbulent flow at a block	12
Figure 4: Flows along a teardrop shape	13
Figure 5: Pressure differences on a wing	13
Figure 6: Downward and upward forces on a wing due to the flow of air	14
Figure 7: The Coanda effect on a wing	14
Figure 8: The angle of attack	15
Figure 9: The lift coefficient as a function of the angle of attack	15
Figure 10: Flow on a wing at a small angle of attack (left) and at a large angle of attack (right)	15
Figure 11: The pitot tube	16
Figure 12: Sketch of a wind tunnel	17
Figure 13: Open wind tunnel	18
Figure 14: a closed wind tunnel	19
Figure 15: structure of the honeycomb	20
Figure 16: the finished honeycomb	20
Figure 17: The funnel with the screens mounted	20
Figure 18: The honeycomb structure of the mosquito net	21
Figure 19: The bending of the funnel we use, the useful domain for us is: $l \in [0.58]$	22
Figure 20: The skeletal structure	23
Figure 21: The inner walls that are folded by weights	23
Figure 22: The finished funnel	23
Figure 23: The finished test section	24
Figure 24: The diffuser	24
Figure 25: Schematic overview of the electronic control of the motors	25
Figure 26: All parts of the fans with a bar of 30 cm in front	26
Figure 27: The pattern in which the holes are cut	26
Figure 28: The legs under the wind tunnel	27
Figure 29: The general setup of the wind tunnel	29
Figure 30: Flow near a bus	29
Figure 31: Current near an old-timer	30
Figure 32: Current near a racing car	30
Figure 33: Illustration of the pitot tube arrangement in the test section	31
Figure 34: Relation of airspeed to fan position	32
Figure 35: The wing arrangement in the test section	33
Figure 36: Measurement of wing angle of attack	34
Figure 37: Wing lift as a function of angle of attack	35
Figure 38: Calculated and experimental lift coefficient as a function of angle of attack	35
Figure 39: Wing lift as a function of wind speed	36

7 List of tables

Table 1: Motor specifications	26
Table 2: Fan components	26
Table 3: Requirements of the components of a wind tunnel	26
Table 4: Location of the pitot tube in the test section	31
Table 5: Determination of homogeneity at maximum fan speed	32
Table 6: Determination of air speed at different fan speeds	32
Table 7: Determination of lift at different angles of attack	34
Table 8: Determination of lift at different airspeeds.	36